Fault Ride Through Capability Enhancement of a Large-Scale PMSG Wind System with Bridge Type Fault Current Limiters

Mohammad Shafiul ALAM, Mohammad Ali Yousef ABIDO
Department of Electrical Engineering, King Fahd University of Petroleum & Minerals, Dhahran, Saudi Arabia
mabido@kfupm.edu.sa

***Abstract*—In this paper, bridge type fault current limiter (BFCL) is proposed as a potential solution to the fault problems of permanent magnet synchronous generator (PMSG) based large-scale wind energy system. As PMSG wind system is more vulnerable to disturbances, it is essential to guarantee the stability during severe disturbances by enhancing the fault ride through capability. BFCL controller has been designed to insert resistance and inductance during the inception of system disturbances in order to limit fault current. Constant capacitor voltage has been maintained by the grid voltage source converter (GVSC) controller while current extraction or injection has been achieved by machine VSC (MVSC) controller. Symmetrical and unsymmetrical faults have been applied in the system to show the effectiveness of the proposed BFCL solution. PMSG wind system, BFCL and their controllers have been implemented by real time hardware in loop (RTHIL) setup with real time digital simulator (RTDS) and dSPACE. Another significant feature of this work is that the performance of the proposed BFCL is compared with that of series dynamic braking resistor (SDBR). Comparative RTHIL implementation results show that the proposed BFCL is very efficient in improving system fault ride through capability by limiting the fault current and outperforms SDBR.**

***Index Terms*—power system faults, energy conversion, wind energy, wind farms, permanent magnet machines.**

I. INTRODUCTION

Electric power demand in the world is increasing progressively as well as there is continuous depletion of fossil fuel. This is motivating system planners to install renewable resource based electric power plants. Maximum power point tracking capability, higher efficiency, independent control of active and reactive power, improved power quality, low maintenance cost of turbine, and no air pollution of wind energy have drawn substantial attention of the researchers among the several renewable energy resources [1–4].

With the intention of enhancement of network reliability, several renewable energy resources are integrated with existing grids [5–7]. In wind energy conversion system mainly two types of wind generators are available: fixed speed wind generator and variable speed wind generator [8–13]. Due to the capability of maximum power point tracking, variable speed wind generation systems have gained widespread attentions of the researchers. Specifically, variable speed wind systems with direct drive permanent magnet synchronous generator (PMSG) are receiving more consideration in wind turbine applications since it has full controllability of the system. In addition, it is gear box free and no need for field excitation [14–16]. As related to doubly fed induction generator (DFIG) wind turbine, PMSG wind turbine has improved proficiency and reliability [17–18].

Fault ride through (FRT) capability and transient stability are the major issues for integration of large scale wind farm to the existing grid. Disturbances in the grid cause instability of such integrated system. The grid faults might initiate disconnection of large-scale wind turbines and wind farms. The sudden disconnection of large-scale power generating units excites the instability of the utility network [19] . A potential solution to stability and security issues is to employ fault current limiter (FCL). Applications of fault current limiters (FCLs) have been widely deliberated in power system to limit fault current as well as improve stability of the system. Generally, superconducting fault current limiter (SFCL) application has been dominant in AC power system [20–23]. In wind energy integrated system, superconducting fault current limiters [24–26] have been studied extensively. The main drawbacks of SFCL are the significant system losses during normal operation and degrading the overall efficiency of wind energy conversion systems [27]. Additionally, [28–30] presented series dynamic braking resistor (SDBR) as a potential solution to limit fault current. SDBR consists of a controllable resistor in parallel with a switch [28]. Depending on the fault appearance, the switch is turned on and turned off to limit the fault current. However, the main drawback of SDBR is that it is highly sensitive to switching delay and shows unsatisfactory performance in limiting fault current and improving transient stability [30].

Among different types of FCLs non-superconducting bridge-type fault current limiter (BFCL) is new technology having the capability of limiting fault current as well as improving dynamic performance of the power grid [31–32]. Diodes and IGBT switch are required for BFCL which can be implemented easily [33]. Moreover, required inductor and resistor for current limiting part of BFCL are non-superconducting in nature. This reduces the implementation cost excessively compared to superconducting fault current limiter. However, this innovative technology has not been examined so far in enhancing FRT capability as well as

This work was supported by Deanship of Scientific Research, King Fahd University of Petroleum & Minerals, through the Electrical Power and Energy Systems Research Group funded project # RG1420-1&2.

Digital Object Identifier 10.4316/AECE.2018.01006

stability of large-scale PMSG based wind energy system, to the best of the authors' knowledge. Since the necessity of auxiliary devices in improving dynamic performance of large-scale PMSG wind system cannot be ignored and cost of application needs to be minimized, BFCL represents a potential solution in this regard. In conclusion, there is a lack of exploring the potential of BFCL to enhance transient stability as well as FRT capability of large-scale PMSG based wind energy system.

This research investigates fault current reduction and FRT capability as well as transient stability enhancement of PMSG based large-scale wind energy system with BFCL. To the best of our knowledge, BFCL has been applied in small-scale DFIG wind systems; however, this advantageous device has not been examined so far in PMSG wind system to enhance system dynamic performance. In this work, the proposed BFCL is compared with the SDBR so as to show the efficacy of BFCL to reduce fault current and improve stability of PMSG based large-scale wind system. BFCL has been placed between point of common coupling (PCC) and grid to limit fault current. The main outcomes of this research are as follows:

- The proposed BFCL has been found as very effective solution in limiting fault current and improving FRT capability of large-scale PMSG wind system during severe disturbances.
- PMSG speed and power oscillations have been damped greatly with BFCL.
- Suppression of DC link voltage fluctuation of the system is observed with the proposed BFCL.
- Another significant feature of this research is that the BFCL performance in PMSG wind system is compared with its counterpart SDBR where BFCL outperforms SDBR in all aspects considered.

II. Bridge Type Fault Current Limiter

In this work, BFCL has been proposed as a potential solution to limit the fault current in PMSG based large-scale wind energy system. Its structure, operation, and control technique are described in the following subsections.

A. BFCL Structure, Operation, and Design Consideration

BFCL is composed of a bridge with a parallel shunt branch [34] as shown in Fig. 1. The bridge part contains four diodes (D_1-D_4), small DC resistor, R_{DC}, and inductor, L_{DC}, with antiparallel diode, and an IGBT switch. The shunt path consists of a series resistance, R_{sh}, and inductance, L_{sh}. The main function of BFCL is to insert the shunt branch impedance in series with the line under the fault conditions to limit the fault current.

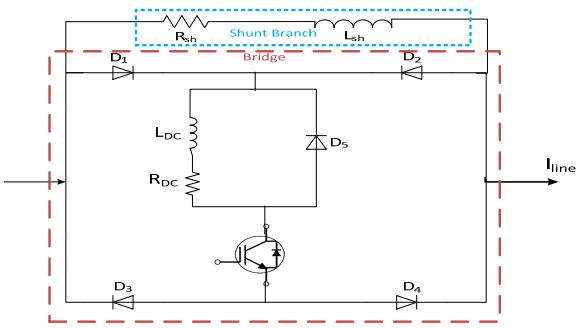

Figure 1. Configuration of bridge type fault current limiter

During the normal system condition, IGBT switch is turned on by its controller. Therefore, for the positive half cycle, current conducts thorough the path D_1-L_{DC}-R_{DC}-*IGBT*-D_4. During the negative half cycle, current passes through the path D_2-L_{DC}-R_{DC}-*IGBT*-D_3. Therefore, the current has a unified direction through L_{DC} and R_{DC}. Consequently, L_{DC} is charged to the peak value of the line current and acts like short circuit. Since the values of R_{DC} and L_{DC} are very small, voltage drop across them is insignificant. Eventually, bridge is short-circuited during normal system operation and it has no effect on the system performance. On the other hand, during system disturbances, IGBT switch is turned off by the BFCL controller. As a result, shunt branch is activated and connected once the bridge part is open. Insertion of the shunt branch impedance during system disturbance limits fault current and improves dynamic stability of PMSG wind system. In this work, BFCL parameters are designed based on the pre-fault power flow through each line. In order to minimize the effect of the fault on the system, BFCL should consume equal or higher amount of active power of pre-fault value. Pre-fault power consumption by the BFCL is given as below [35].

$$P_{BFCL} \le \frac{P_G}{3} \tag{1}$$

$$P_{BFCL} = \frac{V_{PCC}^2 R_{sh}}{R_{sh}^2 + X_{sh}^2} \tag{2}$$

where P_G, $V_{PCC,}$ $R_{sh,}$ and X_{sh} are power delivered to the grid by wind system, voltage at point of common coupling (PCC), shunt resistance, and shunt reactance respectively. Equations (1) and (2) imply: - .

$$P_G R_{sh}^2 - 3V_{PCC}^2 R_{sh} + P_G X_{sh}^2 \ge 0 \tag{3}$$

Above equation gives following equation for R_{sh}

$$R_{sh} \ge \frac{3V_{PCC}^2 + \sqrt{9V_{PCC}^4 - 4P_G^2 X_{sh}^2}}{2P_G} \tag{4}$$

The necessary condition for the R_{sh} to be the real value is that the term inside root must be greater than zero and which gives following equation.

$$X_{sh} < 1.5\frac{V_{PCC}^2}{P_G} \tag{5}$$

The same approach is used to find the value of R_{sh}. For the BFCL to be practical, L_{DC} and R_{DC} are selected some lower values so that the DC current flowing through them is smooth.

B. BFCL Control Technique

Disturbances in AC/DC system can be detected either by voltage dip or over current at the point of common coupling (PCC) [36]. Voltage dip at PCC has been used in this work to detect the fault and generate IGBT gate control pulses as shown in Fig. 2.

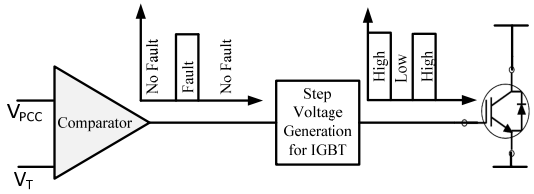

Figure 2. Control strategy of bridge type fault current limiter

A comparator evaluates the level of the PCC voltage (V_{PCC}) with a predefined threshold voltage (V_T) which is considered to be 95% of the nominal V_{PCC}. Under normal operating conditions when V_{PCC} is higher than V_T, comparator output goes on low. Therefore, the step voltage of BFCL controller is high voltage signal to make the IGBT switch on. During grid abnormalities, V_{PCC} decreases and becomes lower than V_T. As a result, the comparator output becomes high. In this condition, low voltage signal is generated by step voltage generation to turn off the IGBT switch. Consequently, shunt branch of BFCL comes into operation to limit fault current and enhance system stability. Once V_{PCC} exceeds V_T due to fault clearance or PCC voltage support by any compensation technique, IGBT receives a high voltage signal and turns on. In this way, BFCL has a negligible effect in normal operating conditions while it inserts a series impedance to limit the fault current and enhance FRT capability of PMSG wind system in abnormal conditions. It is worth mentioning that L_{DC} line current tends to rise drastically during fault initiation. However, L_{DC} limits this current and IGBT switch is protected against high *di/dt*.

III. System Modeling and Controller Design

For transient stability and dynamic performance analysis, PMSG based large-scale wind farm system integrated to grid shown in Fig. 3 is modeled in this work. The Rotor of PMSG is directly driven by horizontal axis variable-speed wind turbine with a gearless drive train. PMSG wind generator is integrated to the utility grid through fully controlled back to back converter system, step-up transformer and filter. Machine side voltage source converter (MVSC) controls the rotor speed to track the maximum power point from the wind turbine. Grid side voltage source converter (GVSC) controls the active and reactive power flow to the grid.

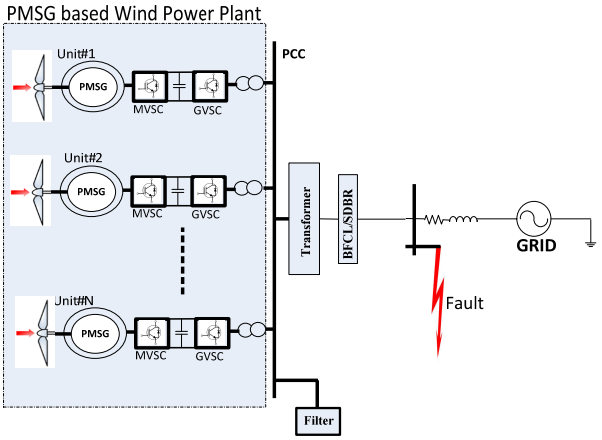

Figure 3. Schematic diagram of PMSG wind system with BFCL/SDBR

A. Wind Turbine Modeling

Generally, operating principle of wind turbine is described by its mechanical power given as [37–38].

$$P_{tur} = 0.5\rho A V_w^3 C_p(\lambda,\beta) \tag{6}$$

where ρ is air mass density in kg/m^3, A is turbine swept area= πr^2, r is turbine radius, V_w is turbine speed in m/s, C_p is the performance coefficient, β is blade pitch angle, and λ is tip speed ratio.

Tip speed ratio is given by the following equation.

$$\lambda = \frac{r\omega_{tur}}{V_w} \tag{7}$$

where ω_{tur} is the turbine angular speed in rad/s. Power delivered by the wind turbine (P_{tur}) can be controlled by varying performance coefficient. Variation of C_p is achieved by varying ω_{tur} and β since wind speed V_w can not be controlled. C_p is highly nonlinear function of β and λ whose analytical expression can be given by the following equation [39].

$$C_p(\lambda,\beta) = \frac{1}{2}(\lambda - 0.022\beta^2 - 5.6)e^{-0.17\lambda} \tag{8}$$

B. Permanent Magnet Synchronous Generator (PMSG) Modeling

Wind energy is extracted and integrated to the grid with PMSG in which field excitation is provided by a permanent magnet. The wind power system utilizes wind turbine which is directly connected to the PMSG rotor. Stator of the PMSG is connected to the point of common coupling (PCC) with AC/DC/AC conversion system with voltage source converters (VSCs). Common DC bus of the VSCs contains a capacitor. The machine is modelled in synchronously rotating *d-q* reference frame aligned to the rotor given as [40].

$$\frac{1}{2}m_d V_{DC} = RI_d + (L_{md} + L_{ls})\frac{dI_d}{dt} - \omega_r(L_{mq} + L_{ls})I_q \tag{9}$$

$$\frac{1}{2}m_q V_{DC} = RI_q + (L_{mq} + L_{ls})\frac{dI_q}{dt} + \omega_r(L_{mq} + L_{ls})I_d + \omega_r\psi_f \tag{10}$$

where d and q are direct and quadrature components respectively, m is the modulation signal, V_{DC} is the DC link voltage, L_{md} and L_{mq} are the mutual inductances, L_{ls} is the stator leakage inductance, I is PMSG stator current, and ψ_f is the permanent magnet flux.

The developed torque has two components: the first component is owing to field flux and the second component is as a result of reluctance torque. The general torque expression is given by the following equation.

$$T_e = 1.5(\hat{\psi}_f I_q + (L_{md} - L_{mq})I_d I_q \tag{11}$$

where $\hat{\psi}_f$ is the peak value permanent flux and T_e is the developed torque. The main reason of using PMSG for harnessing wind energy is that it does not require gearbox and has full controllability of system.

C. Machine Side Voltage Source Converter (MVSC) Controller

MVSC optimally adjusts rotor speed to extract ultimate available power from constantly varying wind speed. The main function of MVSC is to control stator current such that it is 180 degrees out of phase of stator voltage so as to maximize PMSG efficiency. Power generated by the wind turbine over a wide range of speed is measured in order to find optimum rotor speed (ω_{ropt}). Then, corresponding quadrature axis reference current or torque is generated from the measured power by controlling the rotor speed as shown in Fig. 4.

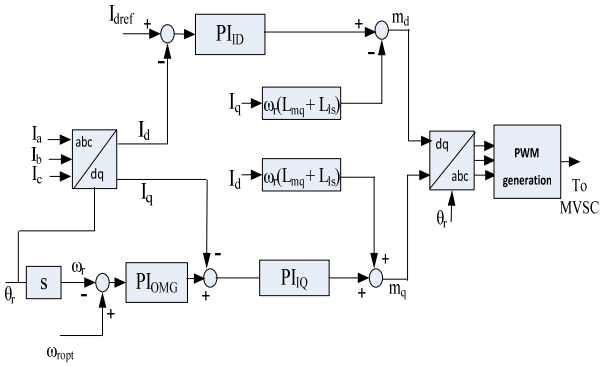

Figure 4. Schematic diagram of controller of MVSC

D. Grid Side Voltage Source Converter (GVSC) Controller

The function of GVSC controller is to regulate active and reactive power exchange between the point of common coupling (PCC) and grid with current control mode inner controllers. Using synchronously rotating *d-q* reference frame, equations describing PCC and GVSC is given as below.

$$\frac{1}{2}m_{dg}V_{DC} = V_{pccd} + R_T I_{dg} - \omega L_T I_{qg} + L_T \frac{dI_{dg}}{dt} \quad (12)$$

$$\frac{1}{2}m_{qg}V_{DC} = V_{pccq} + R_T I_{dg} + \omega L_T I_{dg} + L_T \frac{dI_{qg}}{dt} \quad (13)$$

where m_g is the GVSC modulation index, R_T and L_T are the total resistance and inductance between PCC and grid respectively, and ω is the grid frequency. From the above set of equations, GVSC controller as shown in Fig. 5 is developed. Measured DC link voltage is subtracted from the reference voltage and error is controlled by PI controller providing reference direct axis current. In outer PCC voltage controller, measured PCC voltage is compared with reference PCC voltage and error is controlled by PI controller. Both the *d*-axis and *q*-axis currents provided by the outer controllers are processed with corresponding inner current PI controllers.

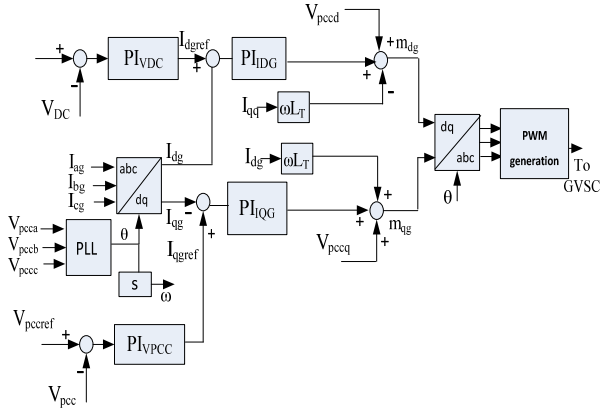

Figure 5. Schematic diagram of controller of GVSC

IV. Results and Discussions

The test system of Fig. 3 is implemented with real time hardware in loop (RTHIL) simulation to validate the effectiveness of proposed BFCL in enhancing the system stability and improving the fault ride through capability. The proposed BFCL is also compared with SDBR to show the improvement of system dynamic performance.

A. System Data and Controller Parameters

Large-scale PMSG wind integrated with BFCL system as shown in Fig. 3 is considered in this work to validate the proposed control strategies. Several PMSG units are connected at the point of common coupling (PCC). The proposed fault current limiting device, BFCL, is connected between PCC and grid as shown in Fig. 3. Outer PI controllers' parameters have been tuned with the symmetrical optimum method [41] while inner PI controllers' parameters have been tuned with pole zero cancellation technique [42]. Detailed PMSG system and controller data are listed in Table I and Table II respectively.

TABLE I. PMSG System Parameters

Parameter	Value
Grid Voltage	33 kV
DC link Voltage	7.6 kV
Stator Voltage	4 kV
Rated power (PMSG)	2 MW
Stator leakage reactance	0.1 pu
Stator resistance	0.01 pu
Rated wind speed	12 m/sec
Coupling transformer	110 MVA, 4/33 kV
Transformer leakage reactance	0.15 pu
DC link capacitance	10 mF
BFCL shunt resistor	10 mΩ
BFCL shunt inductor	2 mH
SDBR resistor	10 mΩ

TABLE II. Controller Parameters

Name	K_p	K_i
PI_{ID}	0.4	8
PI_{IQ}	0.4	8
PI_{OMG}	0.01	2
PI_{VDC}	0.5	50
PI_{VPCC}	10	1000
PI_{IDG}	0.3	7.5
PI_{IQG}	0.3	7.5

B. Real Time Hardware in Loop (RTHIL) Setup with RTDS and dSPACE

RTDS is a fully digital power system simulator that works in real time [43]. It continuously produces output conditions that accurately characterize conditions in the real network by solving the power system equations. Thus, the RTDS has widely been recognized as an ideal tool for the design, development, and testing of power control and protection schemes. The laboratory setup for RTHIL with RTDS and dSPACE is shown in Fig. 6.

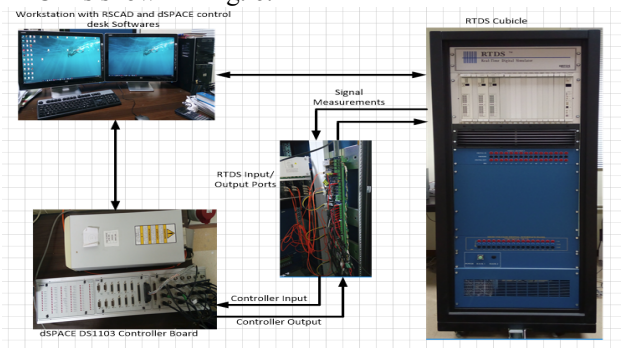

Figure 6. Laboratory setup of real time hardware in loop (RTHIL)

The proposed controllers are developed on dSPACE DS1103 controller board while the RTDS is used for simulation of plant model for large-scale PMSG based wind

system. The RTDS and dSPACE exchange signals by their input/output (I/O) ports. The controllers are implemented using the blocks of dSPACE tool box.

C. RTHIL Simulation Results

Initially, the system operates in its normal condition. Then, the considered system has been tested under symmetrical three-line-to-ground (3LG) and unsymmetrical single-line-to-ground (1LG) faults applied at grid side bus as shown in Fig. 3. The duration of these faults is 6 cycles. Under each fault, three different simulation conditions are tested to show the effectiveness of the proposed BFCL control technique. These conditions are:

- without FCL;
- with SDBR;
- with the proposed BFCL.

Case A: *Symmetrical Fault Application*

At the beginning, system operates in normal operating conditions with a DC link reference voltage of 7.6 kV and reference power delivered to the grid 102 MW. Machine side VSC (MVSC) controller regulates the DC link voltage to 7.6 kV and grid side VSC (GVSC) controller ensures 102 MW power delivery to the grid for a nominal wind speed of 12 m/s. Now, three-line-to-ground (3LG) fault is applied at grid and DC link voltage, active power delivered to the grid, line current, and PMSG speed are presented and compared for both cases of SDBR and the proposed BFCL. Fig. 7 shows the transient response improvement of the system with symmetrical three phase fault applied at grid bus. Fig. 7 (a) shows that the speed of PMSG fluctuates over a wide range without any auxiliary controller. System performance improvement is observed by 19.29% speed fluctuation reduction with SDBR. However, PMSG speed oscillation is greatly damped with the proposed BFCL controller by a fluctuation reduction of 97.24%. Moreover, PMSG speed reaches to its steady state value at 0.8 seconds whereas it takes almost entire simulation time of 2 seconds for both without any auxiliary controller and with SDBR cases. Improvement of system fault ride through capability in terms of DC link voltage oscillation is observed in Fig. 7 (b). DC link voltage fluctuates over a wide range of 5.91 kV to 10.48 kV without any controller. With SDBR, DC link voltage fluctuation is slightly reduced. However, the proposed BFCL controller is superior over SDBR in reducing DC link voltage fluctuation. Settling time for the system without and with SDBR is much higher compared to the proposed BFCL, which greatly reduces settling time for the DC link voltage.

Power delivered to the grid by the PMSG wind system and grid line current are shown in Fig. 8 (a) and (b), respectively for three considered cases under symmetrical three line to ground (3LG) fault applied at grid bus. As shown in Fig. 8 (a) active power oscillates over a wide range without any auxiliary controller. SDBR reduces power oscillation by 25.69%. However, the proposed BFCL solution damps the power oscillation by 48.34%. Moreover, the settling time of the grid power to reach its steady state value with the proposed BFCL is less than the system without and with SDBR. Fig. 8 (b) clearly visualizes the current limiting capability the BFCL over without and with SDBR.

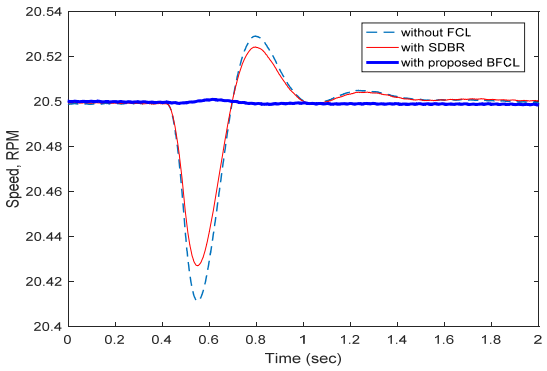

(a)

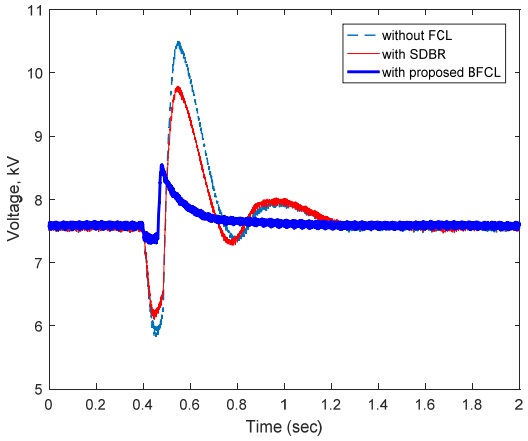

(b)

Figure 7. Comparison of transient response of PMSG wind system subject to symmetrical fault at grid bus (a) PMSG speed (b) DC link capacitor voltage of PMSG wind system

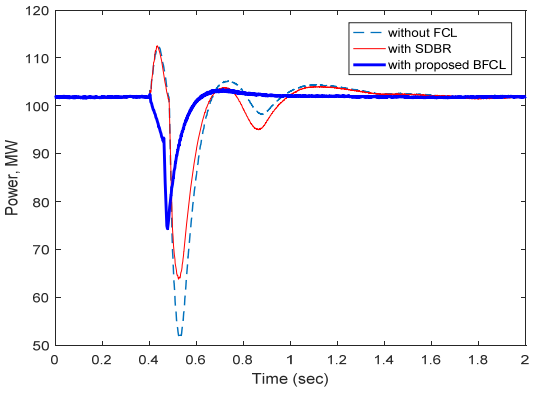

(a)

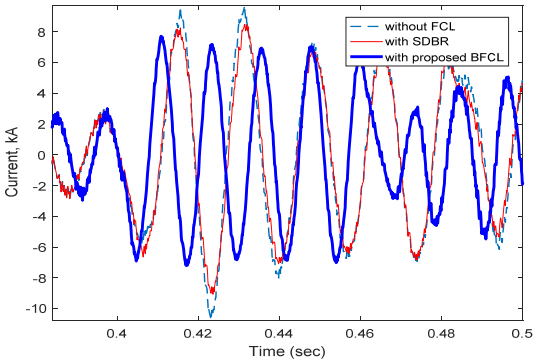

(b)

Figure 8. Comparison of grid side parameters transient response of PMSG wind system subject to symmetrical fault at grid (a) Active power delivery to grid (b) Grid line current

Case B: *Unsymmetrical Fault Application*

Unsymmetrical single-line-to-ground (1LG) fault has been applied at grid bus. RTHIL implementation results in Fig. 9 show clearly the positive effect of the proposed BFCL to reduce PMSG speed oscillation and DC link voltage variation. Fig. 9 (a) shows PMSG speed response of the system with 1LG fault applied at grid. Without FCL, PMSG oscillates over a wide range and it does not reach to the steady state value within the entire simulation period. System performance is slightly improved with SDBR. However, the proposed BFCL greatly improves the system dynamic performance by keeping the PMSG speed oscillation within a narrow range during the fault.

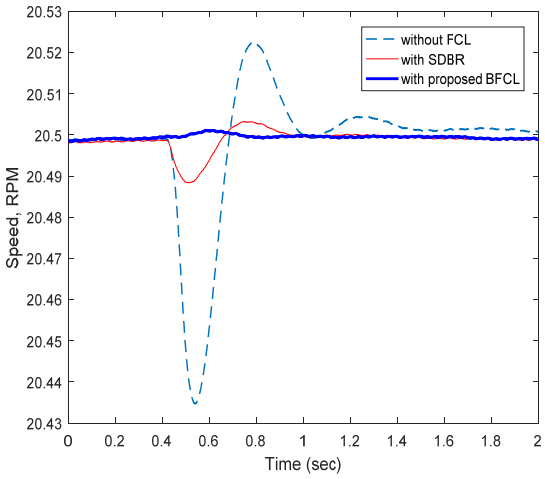

Figure 9. Comparison of transient response of PMSG wind system subject to unsymmetrical fault at grid (a) PMSG speed (b) DC link capacitor voltage of PMSG wind system

Time taken by PMSG speed to reach its reference value is also small for the proposed BFCL compared to without FCL and with SDBR cases. Significant reduction in DC link voltage oscillation is clearly observed with proposed BFCL as shown in Fig. 9 (b).

Improvement in system response in terms of power delivery to grid and line current with the proposed BFCL has been also observed with 1LG fault. Under the fault condition, grid active power delivery and grid current are shown in Fig. 10 (a) and (b) respectively. Fig. 10 (a) shows that the grid power is oscillating over a long period without any auxiliary controller during RTHIL simulation. SDBR reduces power oscillation by only 2.46% while the oscillation has been reduced greatly with the proposed BFCL by 33.62% as observed in the Fig. 10 (a). Fault current limiting capability of the proposed BFCL is visualized in Fig. 10 (b).

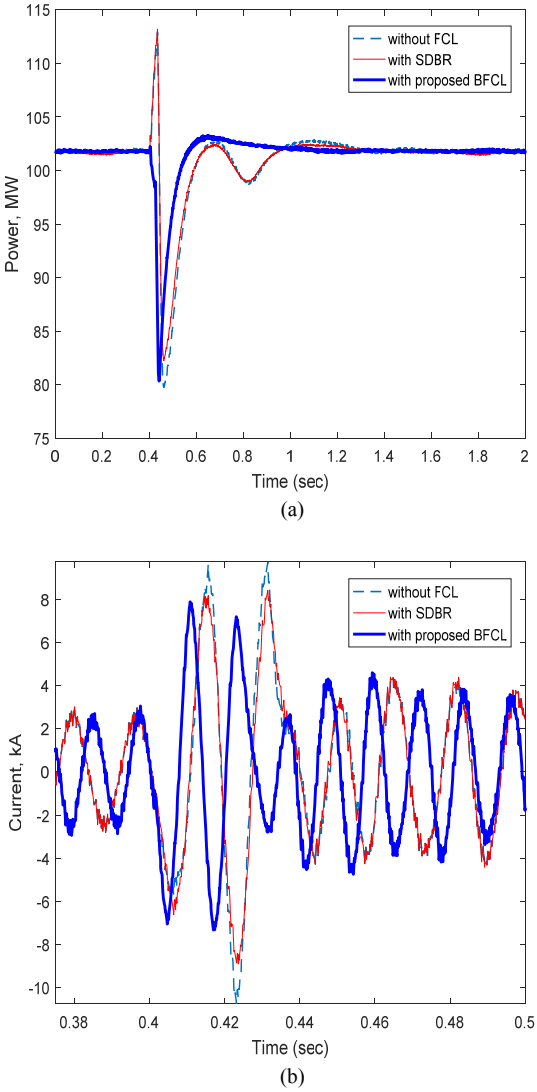

Figure 10. Comparison of grid side parameters transient response of PMSG wind system subject to unsymmetrical fault at grid (a) Active power delivery to grid (b) Grid line current

D. Index-Based Comparison

Besides graphical representations, index-based performance comparison is conducted to get more clear perception of large-scale PMSG wind system performance improvement with the proposed BFCL controller. Several performance indices are considered. These are based on the deviations in DC link voltage, AC power, line current, and PMSG speed. Mathematical expression for the above mentioned indices can be defined as follows:

$$DC_{volt} = \int_0^T |\Delta V_{DC}| dt \tag{14}$$

$$AC_{pow} = \int_0^T |\Delta P| dt \tag{15}$$

$$line_{curr} = \int_0^T |\Delta i| dt \tag{16}$$

$$PMSG_{speed} = \int_0^T |\Delta N| dt \quad (17)$$

where ΔV_{DC}, ΔP, Δi and ΔN represent deviations of DC link voltage, active power flow, line current, and PMSG speed respectively.

TABLE III. PERFORMANCE INDEX IMPROVEMENT WITH PROPOSED BFCL FOR SYMMETRICAL 3LG FAULT

Index %	Without FCL	SDBR	Proposed BFCL
$PMSG_{speed}$	0.074008	0.071551	0.058981
DC_{volt}	0.17706	0.13982	0.041103
AC_{pow}	9.3420	7.8356	3.39930
$line_{curr}$	2.2883	2.2123	2.02560

TABLE IV. PERFORMANCE INDEX IMPROVEMENT WITH PROPOSED BFCL FOR UNSYMMETRICAL 1LG FAULT

Index %	Without FCL	SDBR	Proposed BFCL
$PMSG_{speed}$	0.069471	0.062109	0.057048
DC_{volt}	0.05224	0.045494	0.03457
AC_{pow}	4.0953	3.7037	2.2682
$line_{curr}$	1.9748	1.9512	1.8482

The results in Tables III and IV show that the deviations in all indices considered are much smaller with the proposed BFCL. It can be concluded that stability as well as fault ride through capability of large-scale PMSG wind system have been substantially improved with the proposed BFCL.

V. CONCLUSION

In this work, BFCL has been proposed to limit fault current as well as augment fault ride through capability of large-scale PMSG wind energy system. Depending on fault detection based on PCC voltage, BFCL controller has been designed to insert resistance and inductance during system contingencies in order to limit fault current. Machine side VSC and grid side VSC controllers have been proposed to control DC link capacitor voltage and grid power respectively. Real time hardware in loop simulation of wind turbine, PMSG, and BFCL has been developed with RTDS and dSPACE board DS1103. The effectiveness of the proposed BFCL has been examined through the application of symmetrical as well as unsymmetrical faults. From RTHIL implementation results, BFCL has been found as very effective way of limiting fault current and enhancing dynamic performance of grid integrated large-scale PMSG wind system. The main contributions of this research work can be summarized as:

- The impact of the proposed BFCL solution is substantial in suppressing DC link voltage fluctuation.
- Reduction in fault current, PMSG speed and active power oscillations is achieved with the proposed BFCL control scheme.
- The proposed BFCL solution is superior over SDBR in all aspects as evident from the graphical plots and index based results.

REFERENCES

[1] M. I. Daoud, A. M. Massoud, A. S. A. Khalik, A. Elserougi, and S. Ahmed, "A flywheel Energy storage system for fault ride through support of grid-connected VSC HVDC-based offshore wind farms," IEEE Transactions on Power System, vol. PP, no. 99, pp. 1–10, 2015. doi:10.1109/TPWRS.2015.2465163

[2] E. Rezaei, M. Ebrahimi, and A. Tabesh, "Control of DFIG wind power generators in unbalanced microgrids based on instantaneous power theory," IEEE Transactions on Smart Grid, vol. PP, no. 99, pp. 1–8, 2016. doi:10.1109/TSG.2016.2521644

[3] S. Li and T. A. Haskew, "Energy capture, conversion, and control study of DFIG wind turbine under weibull wind distribution," IEEE Power & Energy Society General Meeting, pp. 1–9, 2009. doi:10.1109/PES.2009.5275870

[4] H. Lund, "Large-scale integration of wind power into different energy systems," Energy, vol. 30, no. 13, pp. 2402–2412, 2005. doi:10.1016/j.energy.2004.11.001

[5] R. G. Lemus, B. G. Díaz, G. Ríos, and R. N. Dib, "Study of the new Spanish legislation applied to an insular system that has achieved grid parity on PV and wind energy," Renewable and Sustainable Energy Review, vol. 49, pp. 426–436, 2015. doi:10.1016/j.rser.2015.04.079

[6] S. Sichilalu, H. Tazvinga, and X. Xia, "Optimal control of a fuel cell/wind/PV/grid hybrid system with thermal heat pump load," Solar Energy, vol. 135, no. 1, pp. 59–69, 2016. doi:10.1016/j.solener.2016.05.028.

[7] M. Ding, Z. Xu, W. Wang, X. Wang, Y. Song, and D. Chen, "A review on China's large-scale PV integration: progress, challenges and recommendations," Renewable and Sustainable Energy Review, vol. 53, pp. 639–652, 2016. doi:10.1016/j.rser.2015.09.009

[8] M. I. Marei, H. S. K. El-Goharey, and R. M. Toukhy, "Fault ride-through enhancement of fixed speed wind turbine using bridge-type fault current limiter," Journal of Electrical Systems and Information Technology, vol. 3, pp. 119–126, 2016. doi:10.1016/j.jesit.2016.01.002

[9] M. Firouzi and G. B. Gharehpetian, "Improving fault ride-through capability of fixed-speed wind turbine by using bridge-type fault current limiter," IEEE Transactions on Energy Conversion, vol. 28, no. 2, pp. 361–369, 2013. doi:10.1109/TEC.2013.2248366

[10] R. Pena, J. C. Clare, and G. M. Asher, "Doubly fed induction generator uising back-to-back PWM converters and its application to variable- speed wind-energy generation," IEE Proceedings on Power Applications, vol. 143, no. 3, pp. 231-241, 1996. doi:10.1049/ip-epa:19960288

[11] D. Kairus, R. Wamkeue, B. Belmadani, and M. Benghanem, "Variable structure control of DFIG for wind power generation and harmonic current mitigation," Advances in Electrical and Computer Engineering, vol. 10, no. 4, pp. 167–174, 2010. doi: 10.4316/AECE.2010.04027

[12] M. Chinchilla, S. Arnaltes, and J. C. Burgos, "Control of permanent-magnet generators applied to variable-speed wind-energy systems connected to the grid," IEEE Transactions on Energy Conversion, vol. 21, no. 1, pp. 130–135, 2006. doi:10.1109/TEC.2005.853735

[13] A. Moghadasi and A. I. Sarwat, "Optimal analysis of resistive superconducting fault current limiters applied to a variable speed wind turbine system," Southeast Conference, pp. 1–7, Florida, USA, 2015. doi:10.1109/SECON.2015.7132944

[14] T. F. Chan and L. L. Lai, "Permanent-magnet machines for distributed power generation: A review," IEEE Power Engineering Society General Meeting, pp. 6–11, 2007. doi:10.1109/PES.2007.385575.

[15] H. Polinder, S. W. H. D. Haan, M. R. Dubois, and J. G. Slootweg, "Basic operation principles and electrical conversion systems of wind turbines," European Power Electronics Drives , vol. 15, no. 4, pp. 43–50, 2005. dx.doi.org/10.1080/09398368.2005.11463604

[16] L. S. Barros, and C. M. V. Barros, "An internal model control for enhanced grid-connection of direct-driven PMSG wind generator," Electric Power System Research, vol. 151, pp. 440-450, 2017. doi.org/10.1016/j.epsr.2017.06.014

[17] H. Li, Z. Chen, and H. Polinder, "Optimization of multibrid permanent-magnet wind generator systems," IEEE Transactions on Energy Conversion, vol. 24, no. 1, pp. 82–92, 2009. doi:10.1109/TEC.2008.2005279

[18] S. Li, T. A. Haskew, R. P. Swatloski, and W. Gathings, "Optimal and direct-current vector control of direct-driven PMSG wind turbines," IEEE Transactions on power electronics, vol. 27, no. 5, pp. 2325–2337, 2012.doi: 10.1109/TPEL.2011.2174254

[19] V. Yaramasu, A. Dekka, M. J. Durán, S. Kouro, and B. Wu, "PMSG-based wind energy conversion systems: survey on power converters and controls," IET Electric Power Applications, vol. 11, no. 6, pp. 956–968, 2017. doi:10.1049/iet-epa.2016.0799

[20] W. T. B. D. Sousa, T. M. L. Assis, A. Polasek, A. M. Monteiro, and R. D. Andrade, "Simulation of a superconducting fault current limiter: A case study in the Brazilian power system with possible recovery

under load," IEEE Transactions on Applied Superconductivity, vol. 26, no. 2, pp. 1–8, 2016. doi:10.1109/TASC.2015.2510609

[21] H. C. Jo and S. K. Joo, "Superconducting fault current limiter placement for power system protection using the minimax regret criterion," IEEE Transactions on Applied Superconductivity, vol. 25, no. 3, pp. 2805-2808, 2015. doi:10.1109/TASC.2015.2411052

[22] S. M. Blair, I. M. Elders, C. D. Booth, G. M. Burt, J. M. Carthy, and N. K. Singh, "Superconducting fault current limiter application in a power-dense marine electrical system," IET Electrical System and Transportation, vol. 1, no. 3, pp. 93-102, 2011. doi:10.1049/iet-est.2010.0053

[23] L. Ye, L. Z. Lin, and K. P. Juengst, "Application studies of superconducting fault current limiters in electric power systems," IEEE Transactions on Applied Superconductivity, vol. 12, no. 1, pp. 900-9003, 2002. doi: 10.1109/TASC.2002.1018545

[24] M. Mardani and S. H. Fathi, "Fault current limiting in a wind power plant equipped with a DFIG using the interface converter and an optimized located FCL," 6th Power Electronics, Drives Systems and Technology Conference, pp. 328–333, 2015. doi:10.1109/PEDSTC.2015.7093296

[25] Y. Zhao, O. Krause, T. K. Saha, and Y. Li, "Stability enhancement in distribution systems with DFIG-based wind turbine by use of SFCL," Australasian Universities Power Engineering Conference, pp. 1-6, 2013. doi:10.1109/AUPEC.2013.6725358

[26] L. Chen, F. Zheng, C. Deng, Z. Li, and F. Guo, "Fault ride-through capability improvement of DFIG-Based wind turbine by employing a voltage-compensation-type active SFCL," Canadian Journal of Electrical and Computer Engineering, vol. 38, no. 2, pp. 132–142, 2015. doi:10.1109/CJECE.2015.2406665

[27] S. Imparato, A. Morandi, L. Martini, M. Bocchi, G. Grasso, M. Fabbri, F. Negrini, and P. L. Ribani, "Experimental evaluation of AC losses of a DC restive SFCL prototype," IEEE Transactions on Applied Superconductivity, vol. 20, no. 3, pp. 1199–1202, 2010. doi:10.1109/TASC.2010.2043726

[28] M. H. Ali and R. A. Dougal, "A closed-loop control based braking resistor for stabilization of wind generator system," IEEE Southeast Conference, pp. 264–267, 2010. doi:10.1109/SECON.2010.5453875

[29] R. Saluja, S. Ghosh, and M. H. Ali, "Transient stability enhancement of multi-machine power system by novel braking resistor models," IEEE Southeast Conference, pp. 3–8, 2013. doi:10.1109/SECON.2013.6567462

[30] A. Causebrook, D. J. Atkinson, and A. G. Jack, "Fault ride-through of large wind farms using series dynamic braking resistors," IEEE Transactions on Power System, vol. 22, no. 3, pp. 966–975, 2007. doi:10.1109/TPWRS.2007.901658

[31] M. A. H. Sadi and M. H. Ali, "A fuzzy logic controlled bridge type fault current limiter for transient stability augmentation of multi-machine power system," IEEE Transactions Power System, vol. 31, no. 1, pp. 602–611, 2016. doi:10.1109/TPWRS.2015.2403258

[32] M. S. Alam, M. A. Y. Abido, "Fault ride-through capability enhancement of voltage source converter-high voltage direct current systems with bridge type fault current limiters," Energies, vol. 10, pp. 1-19, 2017. doi: 10.3390/en10111898

[33] G. Rashid and M. H. Ali, "Bridge-Type Fault current limiter for asymmetric fault ride-through capacity enhancement of doubly fed induction machine based wind generator," IEEE Energy Conversion Congress and Exposition, pp. 1903–1910, 2014. doi:10.1109/ECCE.2014.6953651

[34] M. S. Alam, A. Hussein, M. A. Abido, Z. M. Al-Hamouz, "VSC-HVDC system stability augmentation with bridge type fault current limiter," 6th International Conference on Clean Electrical Power, pp. 531-535, 2017. doi: 10.1109/ICCEP.2017.8004739

[35] G. Rashid and M. H. Ali, "Transient stability enhancement of doubly fed induction machine-based wind generator by bridge-type fault current limiter," IEEE Transactions on Energy Conversion, vol. 30, no. 3, pp. 939–947, 2015. doi: 10.1109/TEC.2015.2400220

[36] X. Liu, P. Wang, and P. C. Loh, "A hybrid AC/DC microgrid and its coordination control," IEEE Transactions on Smart Grid, vol. 2, no. 2, pp. 278–286, 2011. doi:10.1109/TSG.2011.2116162

[37] K. E. Okedu, S. M. Muyeen, R. Takahashi, and J. Tamura "Wind farms fault ride through using DFIG with new protection scheme," IEEE Transactions on Sustainable Energy, vol. 3, no. 2, pp. 242–254, 2012. doi:10.1109/TSTE.2011.2175756

[38] M. M. Hossain, and M. H. Ali, "Transient stability improvement of doubly fed induction generator based variable speed wind generator using DC resistive fault current limiter," IET Renewable Power Generation, vol. 10, no. 2, pp. 1-8, 2015. doi:10.1049/iet-rpg.2015.0150

[39] J. G. Slootweg, H. Polinder, and W. L. Kling, "Representing wind turbine electrical generating systems in fundamental frequency simulations," IEEE Transactions on Energy Conversion, vol. 18, no. 4, pp. 516–524, 2003. doi:10.1109/TEC.2003.816593

[40] N. P. W. Strachan and D. Jovcic, "Stability of a variable-speed permanent magnet wind generator with weak AC grids," IEEE Transactions on Power Delivery, vol. 25, no. 4, pp. 2779–2788, 2010. doi:10.1109/TPWRD.2010.2053723

[41] K. Somsai, T. Kulworawanichpong, and N. Voraphonpiput, "Design of decoupling current control with symmetrical optimum method for D-STATCOM," IEEE Asia-Pacific Power and Energy Conference, pp. 1-4, 2012. doi: 10.1109/APPEEC.2012.6307301

[42] Y. Okada, Y. Yamakswa, T. Yamazaki, and S. Kurosu, "Tuning method of PID controller for desired damping coefficient," IEEE SICE Annual Conference, pp. 795-799, 2007. doi:10.1109/SICE.2007.4421092

[43] S. M. Baek and J. W. Park, "Nonlinear parameter optimization of FACTS controller via real-time digital simulator," IEEE Transactions on Industry Applications, vol. 49, no. 5, pp. 1–8, 2012. doi:10.1109/IAS.2012.6374089